Pseudogaps in the 2D Hubbard Model

C. Huscroft, M. Jarrell, Th. Maier, S. Moukouri, and A. N. Tahvildarzadeh

Department of Physics, University of Cincinnati, Cincinnati, Ohio 45221-0011

(Received 15 October 1999; revised manuscript received 1 June 2000)

We study the pseudogaps in the spectra of the 2D Hubbard model using both finite-size and dynamical cluster approximation (DCA) quantum Monte Carlo calculations. At half-filling, a charge pseudogap, accompanied by non-Fermi-liquid behavior in the self-energy, is shown to persist in the thermodynamic limit. The DCA (finite-size) method systematically underestimates (overestimates) the width of the pseudogap. A spin pseudogap is not seen at half-filling. At finite doping, a divergent d-wave pair susceptibility is observed.

DOI: 10.1103/PhysRevLett.86.139 PACS numbers: 71.10.Fd, 02.70.Lq

Introduction.—For over a decade it has been recognized that the normal state properties of high-T_c superconductors are unusual and appear to have non-Fermi-liquid characteristics [1]. One of the most remarkable features of the normal state is a suppression of the density of states at the Fermi energy in a temperature regime above T_c in underdoped samples. Angular resolved photoemission experiments [2,3] show that this pseudogap in the spectral function has a d-wave anisotropy, the same symmetry as the superconducting order parameter in these materials. This, along with theories that short-range spin fluctuations mediate pairing in the high-T_c cuprates [4,5], emphasizes the importance of understanding the normal state, insulating phase.

It is thought by many that the two-dimensional (2D) Hubbard model, or closely related models, should capture the essential physics of the high-T_c cuprates [4]. Yet, despite years of effort, neither the precursor pseudogap nor d-wave superconducting order have been conclusively seen in the Hubbard model.

Intuitively, one may expect that the Hubbard model should show pseudogap behavior. At half-filling, the ground state of the 2D Hubbard model is an antiferromagnetic insulator [6,7] and the spectrum is therefore gapped. However, the Mermin-Wagner theorem precludes any transition at finite T, so, as the temperature is lowered, one may anticipate that a pseudogap will develop [8]. This question has been previously addressed in the 2D Hubbard insulator by finite-size lattice quantum Monte Carlo (QMC) [9,10] and fluctuation exchange approximation (FLEX) [11] calculations. These results were recently criticized in [12] and are contradictory and inconclusive as to the existence of a pseudogap at low temperatures, due to limitations of these techniques.

By using the recently developed dynamical cluster approximation (DCA) [13,14], we find that at sufficiently low temperatures a pseudogap opens in the single particle spectral weight $A(\mathbf{k}, \omega)$ of the 2D Hubbard model with a simultaneous destruction of the Fermi-liquid state due to short-range antiferromagnetic correlations. This occurs in the weak-to-intermediate coupling regime $U < W$, where U is the on-site Coulomb energy and W is the noninteracting bandwidth. Off half-filling, we see a divergent $d_{x^2-y^2}$ pair susceptibility signaling a finite-T_c onset of superconductivity in the model.

Using finite-size techniques, it is difficult to determine if a gap persists in the thermodynamic limit. At half-filling, finite-size QMC calculations display a gap in their spectra as soon as the correlation length exceeds the lattice size, so they tend to overestimate the pseudogap as it would appear in the thermodynamic limit. Finite-size scaling is complicated by the lack of an exact scaling ansatz for the gap and the cost of performing simulations of large systems. Calculations employing dynamical mean field approximation (DMFA) [15] in the paramagnetic phase do not display this behavior since they take place in the thermodynamic limit rather than on a finite-size lattice. However, the DMFA lacks the nonlocal spin fluctuations often believed to be responsible for the pseudogap. The DCA is a fully causal approach which systematically incorporates nonlocal corrections to the DMFA by mapping the problem onto an embedded impurity cluster of size N_c. N_c determines the order of the approximation and provides a systematic expansion parameter $1/N_c$. While the DCA becomes exact in the limit of large N_c it reduces to the DMFA for $N_c = 1$. Thus, the DCA differs from the usual finite-size lattice calculations in that it is a reasonable approximation to the lattice problem even for a "cluster" of a single site. Like the DMFA, the DCA solution remains in the thermodynamic limit, but the dynamical correlation length is restricted to the size of the embedded cluster. Thus the DCA tends to underestimate the pseudogap.

Method.—The DCA is based on the assumption that the lattice self-energy is weakly momentum dependent. This is equivalent to assuming that the dynamical intersite correlations have a short spatial range $b \lesssim L/2$, where L is the linear dimension of the cluster. Then, according to Nyquist's sampling theorem [16], to reproduce these correlations in the self-energy, we need only to sample the reciprocal space at intervals of $\Delta k \approx 2\pi/L$. Therefore, we could approximate $G(\mathbf{K} + \tilde{\mathbf{k}})$ by $G(\mathbf{K})$ within the cell of size $(\pi/L)^D$ (see Fig. 1) centered on the cluster momentum $\mathbf{K}$ (wherever feasible, we suppress the frequency labels) and use this Green function to calculate the

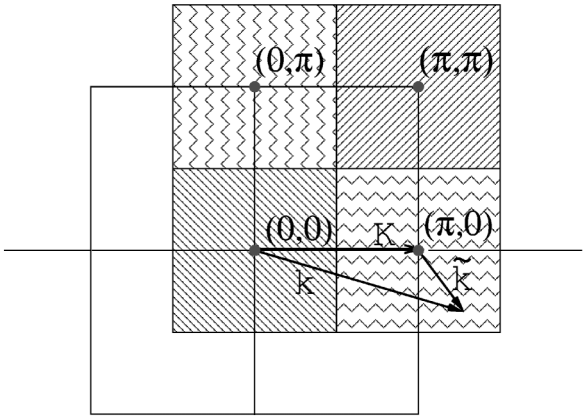

FIG. 1. $N_c = 4$ cluster cells (shown by different fill patterns) that partition the first Brillouin zone (dashed line). Each cell is centered on a cluster momentum $\mathbf{K}$ (filled circles). To construct the DCA cluster, we map a generic momentum in the zone such as $\mathbf{k}$ to the nearest cluster point $\mathbf{K} = \mathbf{M}(\mathbf{k})$ so that $\tilde{\mathbf{k}} = \mathbf{k} - \mathbf{K}$ remains in the cell around $\mathbf{K}$.

self-energy. Knowledge of these Green functions on a finer scale in momentum is unnecessary, and may be discarded to reduce the complexity of the problem. Thus the cluster self-energy can be constructed from the *coarse-grained average* of the single particle Green function within the cell centered on the cluster momenta:

$$\bar{G}(\mathbf{K}) \equiv \frac{N_c}{N} \sum_{\tilde{\mathbf{k}}} G(\mathbf{k} + \tilde{\mathbf{k}}), \tag{1}$$

where N is the number of points of the lattice, N_c is the number of cells in the cluster, and the $\tilde{\mathbf{k}}$ summation runs over the momenta of the cell about the cluster momentum $\mathbf{K}$ (see Fig. 1). For short distances $r \lesssim L/2$, the Fourier transform of the Green function $\bar{G}(r) \approx G(r) + \mathcal{O}[(r\Delta k)^2]$, so that short-range correlations are reflected in the irreducible quantities constructed from $\bar{G}$; whereas, longer-range correlations $r > L/2$ are cut off by the finite size of the cluster [13].

This coarse-graining procedure and the relationship of the DCA to the DMFA is illustrated by a microscopic diagrammatic derivation of the DCA. For Hubbard-like models, the properties of the bare vertex are completely characterized by the Laue function Δ which expresses the momentum conservation at each vertex. In a conventional diagrammatic approach $\Delta(\mathbf{k}_1, \mathbf{k}_2, \mathbf{k}_3, \mathbf{k}_4) = \sum_{\mathbf{r}} \exp[i\mathbf{r} \cdot (\mathbf{k}_1 - \mathbf{k}_2 + \mathbf{k}_3 - \mathbf{k}_4)] = N\delta_{\mathbf{k}_1+\mathbf{k}_2,\mathbf{k}_3+\mathbf{k}_4}$, where $\mathbf{k}_1$ and $\mathbf{k}_2$ ($\mathbf{k}_3$ and $\mathbf{k}_4$) are the momenta entering (leaving) each vertex through its legs of G. However, as $D \to \infty$, Müller-Hartmann showed that the Laue function reduces to [17]

$$\Delta_{D\to\infty}(\mathbf{k}_1, \mathbf{k}_2, \mathbf{k}_3, \mathbf{k}_4) = 1 + \mathcal{O}(1/D). \tag{2}$$

The DMFA assumes the same Laue function, $\Delta_{\mathrm{DMFA}}(\mathbf{k}_1, \mathbf{k}_2, \mathbf{k}_3, \mathbf{k}_4) = 1$, even in the context of finite dimensions. Thus, the conservation of momentum at internal vertices is neglected. Therefore we may freely sum over the internal momenta at each vertex in the generating functional Φ_{DMFA}. This leads to a collapse of the momentum dependent contributions to the functional Φ_{DMFA} and only local terms remain.

The DCA systematically restores the momentum conservation at internal vertices. As discussed above, the Brillouin zone is divided into $N_c = L^D$ cells of size $(2\pi/L)^D$. Each cell is represented by a cluster momentum $\mathbf{K}$ in the center of the cell. We require that momentum conservation is (partially) observed for momentum transfers between cells, i.e., for momentum transfers larger than $\Delta k = 2\pi/L$, but neglected for momentum transfers within a cell, i.e., less than Δk. This requirement can be established by using the Laue function [13]

$$\Delta_{\mathrm{DCA}}(\mathbf{k}_1, \mathbf{k}_2, \mathbf{k}_3, \mathbf{k}_4) = N_c \delta_{\mathbf{M}(\mathbf{k}_1)+\mathbf{M}(\mathbf{k}_3),\mathbf{M}(\mathbf{k}_2)+\mathbf{M}(\mathbf{k}_4)}, \tag{3}$$

where $\mathbf{M}(\mathbf{k})$ is a function which maps $\mathbf{k}$ onto the momentum label $\mathbf{K}$ of the cell containing $\mathbf{k}$ (see Fig. 1).

With this choice of the Laue function the momenta of each internal leg may be freely summed over the cell. This is illustrated for the second-order term in the generating functional in Fig. 2. Thus, each internal leg $G(\mathbf{k}_1)$ in a diagram is replaced by the coarse-grained Green function $\bar{G}[\mathbf{M}(\mathbf{k}_1)]$, defined by Eq. (1). The diagrammatic sequences for the generating functional and its derivatives are unchanged; however, the complexity of the problem is greatly reduced since $N_c \ll N$. We showed previously [13,14] that the DCA estimate of the lattice free energy is minimized by the approximation $\Sigma(\mathbf{k}) \approx \Sigma[\mathbf{M}(\mathbf{k})]$, where $\delta\Phi_{\mathrm{DCA}}/\delta\bar{G} = \bar{\Sigma}$.

The cluster problem is then solved by the usual techniques such as QMC [18], the noncrossing approximation [14], or the fluctuation-exchange approximation. Here we employ a generalization of the Hirsch-Fye QMC algorithm [19] to solve the cluster problem. The initial Green function for this procedure is the bare cluster Green function $\mathcal{G}(\mathbf{K})^{-1} = \bar{G}(\mathbf{K})^{-1} + \Sigma(\bar{\mathbf{K}})$ which must be introduced to avoid overcounting diagrams. The QMC estimate of the cluster self-energy is then used to calculate a new estimate of $\bar{G}(\mathbf{K})$ by using Eq. (1). The corresponding $\mathcal{G}(\mathbf{K})$ is used to reinitialize the procedure which continues until the self-energy converges to the desired accuracy.

Results.—We study the conventional 2D Hubbard Hamiltonian, characterized by an overlap integral t, an on-site

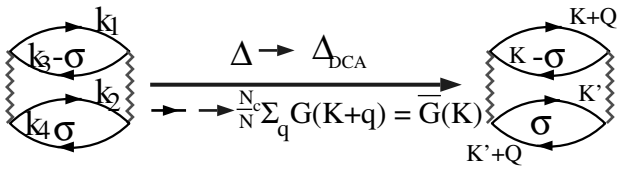

FIG. 2. The DCA choice of the Laue function Eq. (3) leads to the replacement of the lattice propagators $G(\mathbf{k}_1), G(\mathbf{k}_2), \ldots$ by coarse-grained propagators $\bar{G}(\mathbf{K}), \bar{G}(\mathbf{K}'), \ldots$ [Eq. (1)] in the internal legs of Φ_{DCA}, illustrated for a second-order diagram.

potential U, and a chemical potential μ. We set $t = 1$ and measure all energies in terms of t. We work where the system is half-filled, $\langle n \rangle = 1$, and also adjust μ to dope the system to $\langle n \rangle = 0.95$. We choose $U = 5.2$ and 6.0, which are below the value $U \gtrsim W$ believed to be necessary to open a Mott-Hubbard gap.

Figure 3 shows the spectral density $A(\mathbf{k}, \omega)$, and the real $\mathrm{Re}\Sigma(\mathbf{k}, \omega)$ and imaginary $\mathrm{Im}\Sigma(\mathbf{k}, \omega)$ parts of the self-energy for the 2D Hubbard model via the DCA with a paramagnetic host at the Fermi surface X point $\mathbf{k} = (\pi, 0)$ for a 64-site cluster ($N_c = 64$) at various temperatures. We obtain the spectral function $A(\mathbf{k}, \omega)$ via the maximum entropy method [20]. As the temperature is lowered, the system first builds a Fermi-liquid–like peak in $A(\mathbf{k}, \omega)$. By $\beta = 2.6$, a pseudogap begins to develop in $A(\mathbf{k}, \omega)$. The pseudogap builds as the temperature is further lowered. The spectral function $A(\mathbf{k}, \omega)$ at the half-filled Fermi surface point $\mathbf{k} = (\pi/2, \pi/2)$ (not shown) displays qualitative features similar to those seen in Fig. 3, but the pseudogap opens at a slightly lower temperature and the distance between the peaks is less than that seen at the X point.

The DCA self-energy spectra in Fig. 3 support the spectral evidence. At the X point, the slope of $\mathrm{Re}\Sigma(\mathbf{k}, \omega)$ becomes positive below $\beta = 2.6$, the temperature at which we observed the opening of a pseudogap. This signals the appearance of two new solutions in the quasiparticle equation $\mathrm{Re}[\omega - \epsilon_{\mathbf{k}} - \Sigma(\mathbf{k}, \omega)] = 0$ in addition to the strongly damped solution at $\omega = 0$ which is also present in the noninteracting system. These two new quasiparticle solutions for the same $\mathbf{k}$ vector are the consequence of the local moment formation; at low temperatures, the local moments form a short-range antiferromagnetic order which destroys the quasiparticle peak at $\omega = 0$. At these temperatures, $\mathrm{Im}\Sigma(\mathbf{k}, \omega)$ displays a local minimum at $\omega = 0$, indicating the breakdown of the Fermi-liquid behavior.

We also calculate the angle integrated dynamical spin susceptibility shown in the inset. It does not have a pseudogap, as expected for the half-filled model, since the spin-wave spectrum is gapless. Since a (spin) charge gap is generally defined as one which appears in the (spin) charge dynamics, we conclude that the pseudogap is only in the charge response and is due to short-range antiferromagnetic spin correlations.

Figure 4 shows the spectral density $A(\mathbf{k}, \omega)$ at $\mathbf{k} = (\pi, 0)$ and $\mathbf{k} = (\pi/2, \pi/2)$ with $T = 0.06$, $U = 6.0$, $N_c = 8$, and a filling of $\langle n \rangle = 0.95$. Once again, a pseudogap opens in $A(\mathbf{k}, \omega)$, but in this case the pseudogap is highly asymmetric. The inset of Fig. 4 shows the $d_{x^2-y^2}$ pair susceptibility and the magnetic susceptibility as a function of T. T_c occurs where the pair susceptibility diverges, with $T_c \approx 0.04$. This d-wave superconductivity persists in simulations of larger clusters. However, due to the computational cost of these large cluster simulations, we have not completed a systematic study of the effect of system size on the superconducting T_c. This will be the subject of a later study.

The inset of Fig. 4 also shows a sharp drop in the magnetic susceptibility at roughly the temperature where the pseudogap opens, as seen experimentally in the cuprates [1]. In order to ascertain whether this is a signal of pairing,

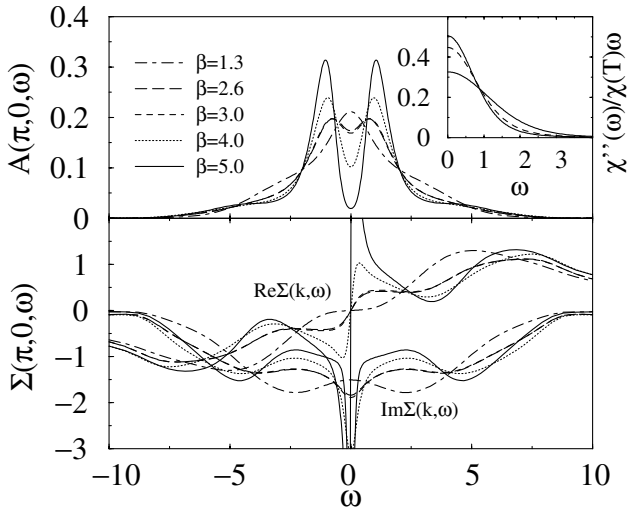

FIG. 3. The spectral density $A(\mathbf{k}, \omega)$, and the real $\mathrm{Re}\Sigma(\mathbf{k}, \omega)$ and imaginary $\mathrm{Im}\Sigma(\mathbf{k}, \omega)$ parts of the self-energy for the 2D Hubbard model via the DCA with a paramagnetic host at $\mathbf{k} = (\pi, 0)$ for a 64-site cluster ($N_c = 64$) at various temperatures. The on-site Coulomb repulsion $U = 5.2$, the bandwidth $W = 8$, and the filling $\langle n \rangle = 1$. As the temperature is lowered, the system first builds a Fermi-liquid–like peak in $A(\mathbf{k}, \omega)$. By $\beta = 2.6$, a pseudogap begins to develop in $A(\mathbf{k}, \omega)$ and, simultaneously, $\mathrm{Re}\Sigma(\mathbf{k}, \omega)$ develops a positive slope at $\omega = 0$, a signal of a non-Fermi liquid. The pseudogap deepens as the temperature is further lowered. The imaginary part of the dynamic spin susceptibility, divided by the static spin susceptibility is shown in the inset. No spin gap is seen.

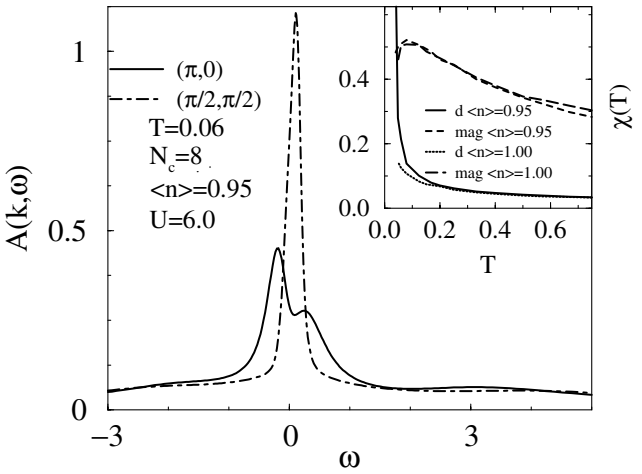

FIG. 4. The spectral density $A(\mathbf{k}, \omega)$ at $\mathbf{k} = (\pi, 0)$ and $\mathbf{k} = (\pi/2, \pi/2)$ with $T = 0.06$, $U = 6.0$, $N_c = 8$, and $\langle n \rangle = 0.95$. The inset shows the $d_{x^2-y^2}$ pair susceptibility (d) and the magnetic susceptibility (mag) as a function of T. The pair susceptibility diverges at a finite T_c. The magnetic susceptibility drops suddenly when the pseudogap opens.

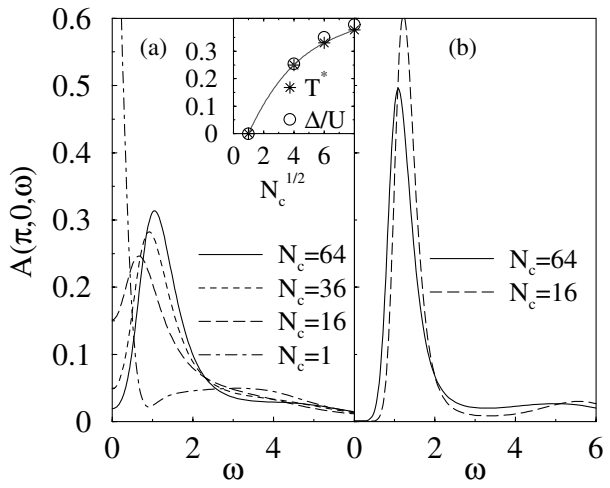

FIG. 5. The spectral density $A(\mathbf{k},\omega)$ at $\mathbf{k} = (\pi, 0)$ for the 2D Hubbard model via (a) the DCA and (b) finite-size quantum Monte Carlo at an inverse temperature times the bandwidth $\beta W = 40$, $U = 5.2$, and a filling $\langle n \rangle = 1$ on various size clusters. The temperature T^* at which the pseudogap first becomes apparent in the DCA spectra, as well as the full width Δ/U measured from peak to peak divided by U, is plotted in the inset. The finite-size QMC overestimates Δ/U and T^*, whereas the DCA QMC systematically underestimates them.

we examine the magnetic susceptibility in the $\langle n \rangle = 1$ model. We see striking downturns at both half-filling and off half-filling. Since the pair-field susceptibility at $\langle n \rangle = 1$ displays no evidence of a finite-T divergence, we infer that a downturn in the magnetic susceptibility at low-T is due to short-range antiferromagnetic order, not the formation of pairs.

It is instructive to compare the DCA results with those obtained by finite-size QMC calculations. Figure 5 shows the spectral density $A(\pi, 0, \omega)$ obtained by analytically continuing both finite-size and DCA QMC data for $\langle n \rangle = 1$. In spite of the difference in the two methods, the information they provide is complimentary. In the finite-size results [Fig. 5(b)], we see a similar opening of a pseudogap. However, as the antiferromagnetic (AF) correlations extend to the longest length on the finite-size lattice, the system develops a full gap. Thus, the finite-size QMC overestimates the size of the gap. In the DCA results [Fig. 5(a)], the pseudogap emerges as soon as $N_c > 1$. The temperature T^* at which the pseudogap first becomes apparent in the spectra, as well as the full width Δ/U measured from peak to peak, is plotted in the inset. Both T^* and Δ/U increase with N_c. Since the DCA calculation remains in the thermodynamic limit, a full gap due to antiferromagnetic correlations alone cannot open until their correlation length diverges. However, some combination of Mott and AFM mechanisms could open a finite-T gap. This will be the subject of a future publication. However, since these correlations are restricted to the size of the cluster, the DCA systematically underestimates the size of the gap. Thus, if a pseudogap exists in the DCA for finite N_c, it should persist in the limit as $N_c \to \infty$.

In summary, we have employed the recently developed DCA to study the long-open question of whether the half-filled Hubbard model has a pseudogap due to AF spin fluctuations. We find conclusive evidence of a pseudogap in the charge dynamics and have shown unambiguously that the $T = 0$ phase transition of the half-filled model is preceded by an opening of a pseudogap in $A(\mathbf{k}_F, \omega)$ accompanied by pronounced non-Fermi-liquid behavior in $\Sigma(\mathbf{k}_F, \omega)$. Off half-filling, the pseudogap becomes highly anisotropic and is accompanied by a d-wave pairing instability. We note that Lichtenstein *et al.* [21] also use the DCA with QMC to study the phase diagram of the 2D Hubbard model. However, they modify the DCA by interpolating the self-energy between the K points. As noted previously [13], this can yield causality violations.

We acknowledge useful conversations with P. van Dongen, B. Gyorffy, M. Hettler, H. R. Krishnamurthy, R. R. P. Singh, and J. Zaanen. This work was supported by the National Science Foundation, Grants No. DMR-9704021, No. PHY94-07194, and No. DMR-9357199, and the Ohio Supercomputing Center.

[1] For reviews, see M. B. Maple, J. Magn. Magn. Mater. **177–181**, 18 (1998); J. L. Tallon and J. W. Loram, Physica C (to be published), cond-mat/0005063.
[2] H. Ding *et al.,* Nature (London) **382**, 51 (1996).
[3] F. Ronning *et al.,* Science **282**, 2067 (1998).
[4] For a review, see D. J. Scalapino, cond-mat/9908287.
[5] T. Timusk and B. Statt, Rep. Prog. Phys. **62**, 61 (1999).
[6] J. E. Hirsch, Phys. Rev. B **31**, 4403 (1985).
[7] S. R. White *et al.,* Phys. Rev. B **40**, 506 (1989).
[8] A. P. Kampf and J. R. Schrieffer, Phys. Rev. B **41**, 6399 (1990).
[9] M. Vekic and S. R. White, Phys. Rev. B **47**, 1160 (1993).
[10] C. E. Creffield *et al.,* Phys. Rev. Lett. **75**, 517 (1995).
[11] J. J. Deisz, D. W. Hess, and J. W. Serene, Phys. Rev. Lett. **76**, 1312 (1996).
[12] S. Moukouri *et al.,* Phys. Rev. B **61**, 7887 (2000).
[13] M. H. Hettler *et al.,* Phys. Rev. B **58**, 7475 (1998); M. H. Hettler *et al.,* Phys. Rev. B **61**, 12 739 (2000).
[14] Th. Maier *et al.,* Eur. Phys. J. B **13**, 613 (2000).
[15] W. Metzner and D. Vollhardt, Phys. Rev. Lett. **62**, 324 (1989).
[16] D. F. Elliot and K. R. Rao, *Fast Transforms: Algorithms, Analyses, Applications* (Academic Press, New York, 1982).
[17] E. Müller-Hartmann, Z. Phys. B **74**, 507 (1989).
[18] S. Moukouri *et al.,* (to be published).
[19] J. E. Hirsch and R. M. Fye, Phys. Rev. Lett. **56**, 2521 (1986).
[20] M. Jarrell and J. E. Gubernatis, Phys. Rep. **269**, 135 (1996).
[21] A. I. Lichtenstein and M. I. Katsnelson, cond-mat/9911320.